EVALUATION OF U-RANS PERFORMANCE IN PREDICTING AN UNCONFINED SWIRLING FLOW WITH PRECESSING VORTEX CORE BASED ON LES AND EXPERIMENTS

B. Wegner*, A. Maltsev, C. Schneider, A. Sadiki, A. Dreizler and J. Janicka
Chair of Energy and Powerplant Technology,
Department of Mechanical Engineering,
Darmstadt University of Technology,
Petersenstr. 30, 64287 Darmstadt, Germany
*bwegner@ekt.tu-darmstadt.de

ABSTRACT

Swirl flows play an important role in many engineering applications such as modern gas turbines, aero propulsion systems etc. While the enhanced mixing and stabilisation of the flame caused by the swirl are desirable features, such flows often exhibit hydrodynamic instabilities called precessing vortex core. For design purposes it is very important to predict such instabilities. Computational fluid dynamics (CFD) using Reynolds-averaged Navier-Stokes (RANS) type turbulence models are state of the art for the prediction of flow properties in engineering practice.

The objective of this paper is therefore to evaluate the performance of the unsteady RANS (U-RANS) method in predicting the precessing vortex core phenomenon. To this end, an unconfined swirl flow with precessing vortex core at Swirl number 0.75 and Reynolds number ranging from 10 000 to 42 000, investigated by means of both experiments and large eddy simulation, is utilised.

INTRODUCTION

Swirling motion in fluid flow has been used for many decades in a broad range of engineering applications. Many studies have been performed on swirl-burners due to their widespread use in combustion systems. In these systems, enhanced mixing and stabilisation of the flame are beneficial phenomena associated with swirl. Reviews on the topic have been given by Syred and Beer (1974), Leibovich (1978), Gupta et al. (1984) and recently by Lucca-Negro and O'Doherty (2001). Chanaud (1965) reported periodic vortex instabilities associated with the swirl in a certain regime of Reynolds and swirl numbers. Since then the so called precessing vortex core (PVC) phenomenon has been paid much attention. It has been observed in premixed combustion systems that the oscillations of the precessing vortex core can amplify and cause a feedback mechanism with acoustic modes of the system. This poses a problem as lean premixed combustion is becoming more and more popular due to it's potential of low-NOx production. Therefore models and simulation methods used in combustor design must be able to predict the precessing vortex core.

For the numerical prediction of flow properties in engineering practice RANS type turbulence models are state of the art. This is mostly motivated by reasonable computational costs required by this method. A review on the application of RANS models to swirl flows has been given by Sloan et al. (1986). Many studies have shown that the $k-\varepsilon$ and other two-equation models in general perform poor due to their deficiencies in the presence of strong streamline curvature. Reynolds stress models (RSM) proved to be better suited for the prediction of swirl flows. For a recent review on RANS/U-RANS in general, see Durbin (2002).

Most RANS computations of swirl flows in the past have been performed assuming axisymmetry and therefore using 2-d computational grids. Since swirl flow instabilities are 3-dimensional and time dependent in nature, their numerical prediction is computationally expensive and has been attempted only recently. Bowen et al. (1998) achieved qualitative agreement with experimental data for swirl-burner furnace system using a Reynolds stress model. They set asymmetric initial conditions from which the PVC ensued, but was damped out after a few revolutions. The precession frequency was predicted within 20% of the value observed in experiments. Guo et al. (2002) employed a $k-\varepsilon$-model to a low-swirl flow in a sudden expansion chamber. They observed several modes of vortex core oscillation. A comparison with experimental results was not given in this work.

In the last few years, large eddy simulation (LES) has been successfully used by several authors to predict swirling flows with or without unsteady phenomena. Pierce and Moin (1998) achieved excellent results in predicting swirled coaxial jets. Derksen and den Akker (2000) accurately captured the PVC phenomenon performing LES of a cyclone. Recently, Tang et al. (2002) obtained encouraging results applying LES to the simulation of an isothermal swirl flow with recirculation. Düsing et al. (2002) used LES to investigate the influence of oscillating inflow conditions on a swirled, non-premixed combustor. This motivates the use of LES results for validation purposes in U-RANS modelling besides experimental data or where such data are not available.

The present study focuses on an evaluation of the performance of U-RANS simulations in predicting an unconfined swirling flow with a precessing vortex core. The flow under consideration has been studied in house by means of experiments which are complemented by LES of the same flow.

MODELLING AND COMPUTATIONAL METHOD

For both the U-RANS and the LES approach the time dependent three dimensional continuity and Navier-Stokes equations are considered for the incompressible case

$$\frac{\partial \overline{u}_i}{\partial x_i} = 0 \tag{1}$$

$$\frac{D\overline{u_i}}{Dt} = \frac{\partial}{\partial x_j}\left(\overline{\nu}\frac{\partial \overline{u_i}}{\partial x_j} - \tau_{ij}\right) - \frac{1}{\varrho}\frac{\partial \overline{p}}{\partial x_i} \tag{2}$$

The overbar denotes the Reynolds averaging and spatial filtering operators for the U-RANS and LES respectively. The

turbulent stress tensor τ_{ij} appearing as an unclosed term on the r.h.s. of equation 2 has to be modelled. In the frame work of RANS $\tau_{ij} = \overline{u_i' u_j'}$ is called the Reynolds stress tensor whereas it is called the subgrid-scale stress tensor defined as $\tau_{ij} = \overline{u_i u_j} - \overline{u_i}\,\overline{u_j}$ for LES.

U-RANS modelling

It has been claimed in the past that RANS cannot be applied to unsteady flows unless there is a spectral gap between the unsteadiness and the turbulence. As pointed out by Durbin (2002) this is based on the misconception that Reynolds averaging equals temporal averaging. If statistical periodicity is defined via the existence of a narrow peak representing the unsteadiness of the flow in the spectrum there is no need for a spectral gap. The peak can occur right in the midst of the broadband turbulent scales and Reynolds averaging is simply interpreted as phase averaging.

A second-order closure has been chosen here for it's well-known capability to well predict swirl flows. Hence, the transport for the components of the Reynolds stress tensor has to be solved.

$$\begin{aligned}\frac{D\overline{u_i' u_j'}}{Dt} = & \underbrace{\frac{\partial}{\partial x_k}\left(-\overline{u_k' u_i' u_j'} - \frac{1}{\varrho}\overline{p' u_i'}\delta_{jk} - \frac{1}{\varrho}\overline{p' u_j'}\delta_{ik}\right)}_{T_{ijk}} \\ & \underbrace{- \left(\overline{u_i' u_k'}\frac{\partial \overline{u_j}}{\partial x_k} + \overline{u_j' u_k'}\frac{\partial \overline{u_i}}{\partial x_k}\right)}_{P_{ij}} \\ & \underbrace{+ \overline{\frac{p'}{\varrho}\left(\frac{\partial u_i'}{\partial x_j} + \frac{\partial u_i'}{\partial x_j}\right)}}_{\Pi_{ij}} \underbrace{- 2\nu \overline{\frac{\partial u_i'}{\partial x_k}\frac{\partial u_j'}{\partial x_k}}}_{\varepsilon_{ij}}\end{aligned} \tag{3}$$

For the turbulent transport term T_{ijk} the model of Shir (1973) is applied. The production term P_{ij} does not contain any unclosed expressions. The linear model of Jones (1994) is applied to model the pressure-strain correlation tensor Π_{ij}. The dissipation term ε_{ij} in (3) is modelled by assuming local isotropy of the small scales. A separate transport equation is solved for ε. Here, the model of Shir (1973) is again applied to the turbulent transport.

Other RSM were also tried out in the course of this investigation, but did not give the same quality of results as the formulations described above.

LES modelling

For the LES a Smagorinsky-model with dynamic procedure according to Lilly (1992) was used to describe the influence of the small scales on the resolved ones. The filtering operation is performed implicitely by means of the finite-volume discretisation. No special wall-treatment is included in the subgrid-scale model.

Computational Method

The same CFD code was used for both U-RANS and LES calculations. The governing equations were dicretised on a block-structured boundary-fitted collocated grid following the finite-volume approach. Spatial discretisations are $2nd$ order with a flux blending technique for the convective terms. The solution is forwarded in time using the $2nd$ order accurate implicit Crank-Nicolson scheme. A SIMPLE type pressure correction method is used for pressure-velocity coupling. The resulting set of linear equations are solved iteratively. Details on the method can be found in the paper by Mengler et al. (2001).

For the U-RANS computations, a flux blending parameter $\alpha = 0$ (i.e. pure $1st$ order upwind differencing) was used to ensure stability of simulations. All the LES were run with almost pure central differencing ($\alpha = 0.95$). The time step width was chosen to give a CFL number of the order of 5 for the U-RANS. For the LES the time step width was smaller by a factor of 10 to resolve all the fluctuations of the grid-scale eddies.

EXPERIMENTAL AND NUMERICAL SETUP

The flow configuration investigated in this paper is based on a non-premixed swirl-burner that has been extensively studied in the well-known TECFLAM-project (see e.g. Schneider et al. (2001)). Recently, the setup has been changed to investigate length and time scales in premixed combustion. A set of isothermal air flow measurements have also been performed in the course of this investigation which are used within this paper.

The experimental setup consists of a movable block type swirler which feeds an annulus from which the air flow enters the measurement section at ambient pressure and temperature. The Reynolds number is computed from the bulk velocity and bluff-body diameter. Three cases were investigated experimentally in which the (geometrical) swirl number was set to $S = 0.75$. Two cases were selected for this paper which will be referred to as the $30kW$ and $150kW$ cases (according to the thermal power for premixed operation of the burner). The Reynolds numbers Re and mass flow rates $\dot{V}$ of the two cases are given in table 1. A

Table 1: The two cases investigated in this paper

	$30kW$	$150kW$
Re	10 000	42 000
$\dot{V}\ [m^3/h]$	35.54	174.55

coflow of 0.5 m/s surrounds the swirler device. A sketch of the device is given in figure 1. Single-point measurements were performed with a TSI 2d-LDV setup that was used in backscatter mode to determine two velocity components at a time. Magnesium oxide particles of less than 1 μm diameter were used to seed the flow. For the evaluation

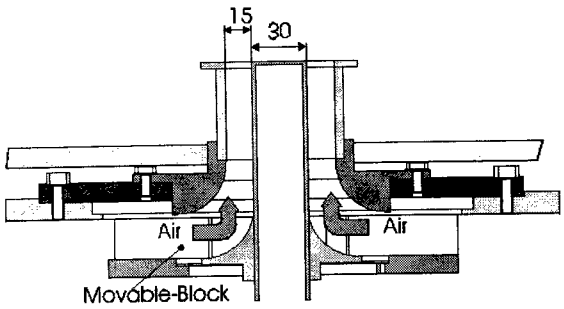

Figure 1: Sketch of the swirler device and dimensions.

of mean values and fluctuations roughly 10 000 events were sampled. The overall error for the experimental data is estimated to be within 3% for the mean values and 7% for fluctuations. Two-point measurements were also performed

where one probe was kept fixed while the other probe was traversed. All the samples collected with the fixed probe (a total of $1.5 \cdot 10^6$!) went into the computation of the temporal autocorrelation and power spectral density which was used to determine the vortex core frequency. The two-point correlations computed from the data collected thus are not presented in this paper.

The computational domain for both the U-RANS and LES consisted of approximately 500 000 control volumes and was shaped cylindrically. It was 600 mm long with a diameter of 600 mm. Free slip boundary conditions were applied to the lateral boundaries and a zero gradient outflow condition was set for the face surface. First simulations were performed with the inlet boundary being flush with the swirler exit plane, prescribing experimental data taken at 1 mm above the swirler exit as inlet boundary conditions. No satisfying results could be obtained though by doing so. Therefore the swirler device was included in the computational domain. Hence, the inlet boundary was moved to the inlet channels of the swirler device. A picture of the grid that was used to model the swirler is given in figure 2.

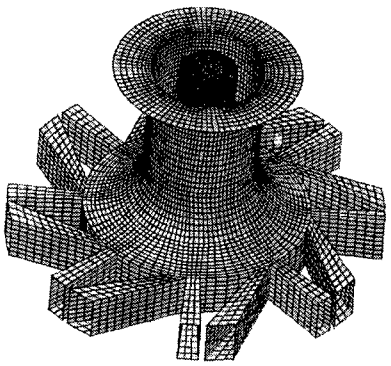

Figure 2: The computational grid used to model the movable block swirler device.

Since the swirler device is fed from a plenum chamber, a constant radial inflow velocity was set on the inlet boundary which was adjusted to result in the correct mass flow for the two cases.

RESULTS AND DISCUSSION

Flow Structure

Due to the single-point nature of the LDV technique, no information about instantaneous flow structures could be obtained from the experimental data. This kind of information can be obtained from the LES. Figure 3 shows instantaneous snapshots from the LES flow field covering one revolution of the precessing vortex core. The flow features that can be observed are:

- The central reverse flow zone performs a precession motion around the bluff-body of the swirler device.
- The recirculation reaches upstream into the swirler device. This explains why the first simulations performed without the swirler failed to predict any unsteady behavior of the flow.
- Two opposed helical vortices shed off the outside edge of the swirler exit. They rotate with the same frequency as the recirculation bubble.

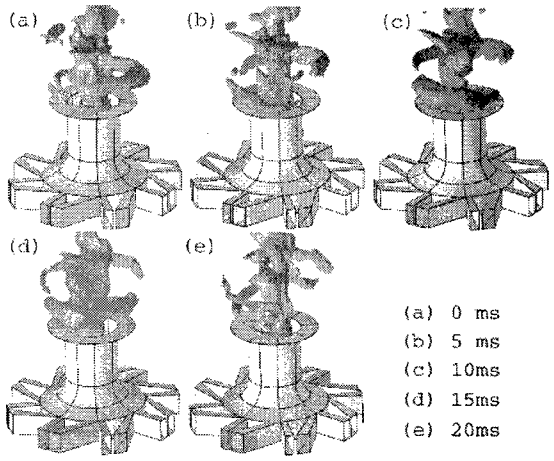

Figure 3: Isosurfaces of instantaneous axial velocity $u = -0.5m/s$ taken from the LES of case $30kW$ showing the flow structure covering one revolution of the vortex core. (taken from Wegner et al. (2003))

As is shown by figure 4, the U-RANS clearly captures the precessing vortex core: a rotating movement of the vortex centre about the system's geometrical axis can be observed. It is noteworthy that no converged stationary solution could be obtained which also indicates the unsteady nature of the flow under consideration.

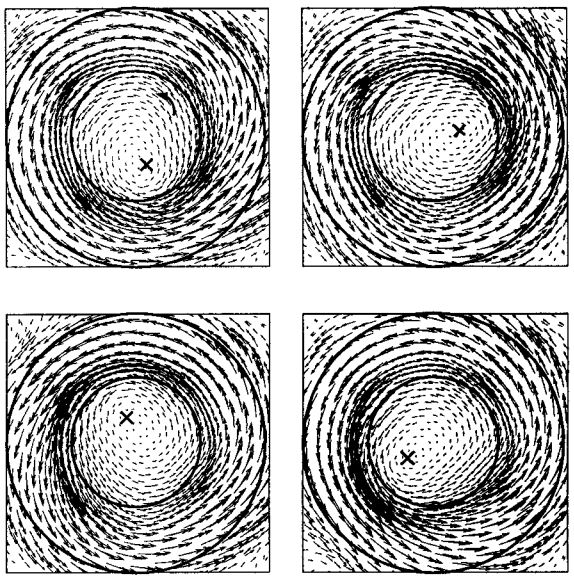

Figure 4: Sequence of snapshots (top left to bottom right) taken from the U-RANS of the $30kW$ case showing vector plots of velocity in a plane $x = 30mm$. The swirler annulus is indicated by the two concentric circles. The approximate instantaneous vortex centre and precession direction are also indicated.

Velocity and Fluctuation Profiles

Radial profiles of time averaged axial and azimuthal velocity as well as the turbulent kinetic energy for both cases are shown in figures 5-10. Both LES and U-RANS simulations capture the experimental mean velocity profiles quite well. Near the swirler exit the RSM gives even better results

than the LES. This can be explained by the coarse grid resolution in the swirler device (only 8 cells were used to resolve the radial direction of the annulus). This is by far not fine enough for the LES to cover the near wall behavior of the flow. The plots of kinetic energy support this as the peak fluctuations at the swirler exit are located in the annulus middle. Due to the wall-induced shear they should be near the wall. Since the RSM includes a wall-model it has got an advantage here.

The results obtained with the U-RANS for the kinetic energy are much too low when compared to the experiments. This is more pronounced for the $150kW$ case. The LES predicts the correct level of kinetic energy and also captures a good deal of the profile shapes.

As the plots of axial velocity indicate, the length of the recirculation zone is also well-predicted by the U-RANS. When one looks at the radial peak positions of axial velocity it seems that the expansion rate of the flow is underpredicted by the U-RANS when compared to the LES and experiments. This is also more pronounced in the $150kW$ case and might be linked to the underprediction of kinetic energy that was mentioned above. A possible explanation is that the intensity of the precessing vortex is underpredicted by the RSM. The use of phase averaging could help answer this question, but would go beyond the scope of this paper.

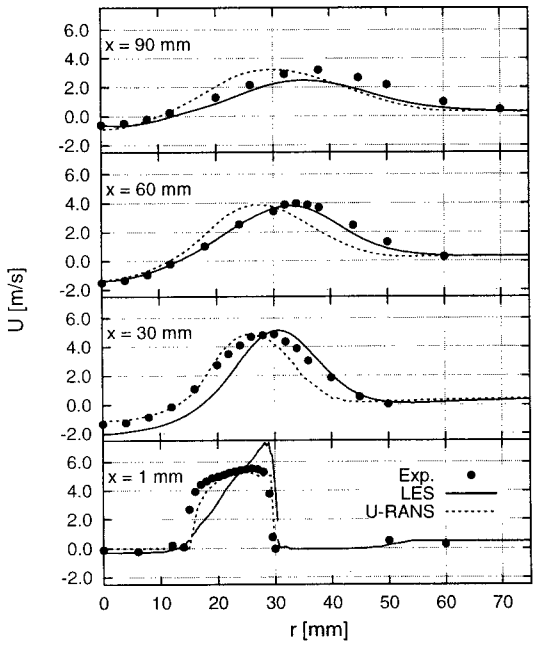

Figure 5: Radial profiles of time averaged axial velocity at several axial positions for the $30kW$ case.

Precession frequency

For both the experiment and the LES, the vortex core precession frequency was obtained from the turbulent energy spectrum as computed from temporal autocorrelations. As can be seen in figure 11 the spectra show distinct peaks associated with the motion of the vortex core. Furthermore, these spectra show a second weaker peak at the doubled PVC frequency. This peak is associated with the opposed helical vortices that are shown by the LES. Since they perform a rotating motion at the same speed as the central recirculation, the monitoring point (at which the velocity time series for the spectral analysis was sampled) is passed twice by such a

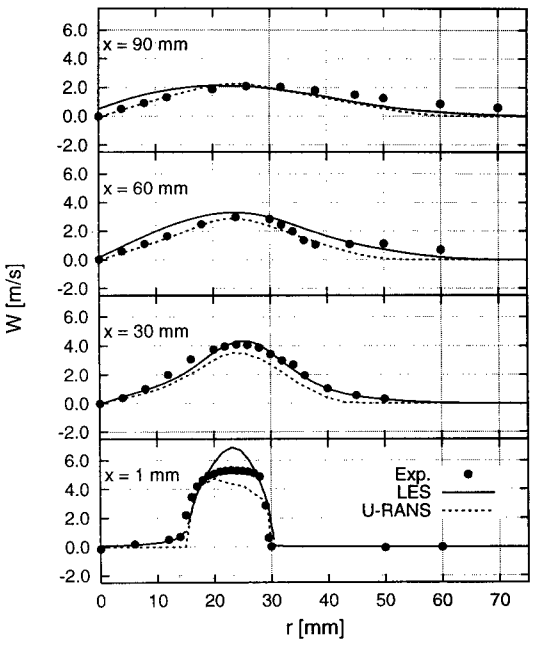

Figure 6: Radial profiles of time averaged azimuthal velocity at several axial positions for the $30kW$ case.

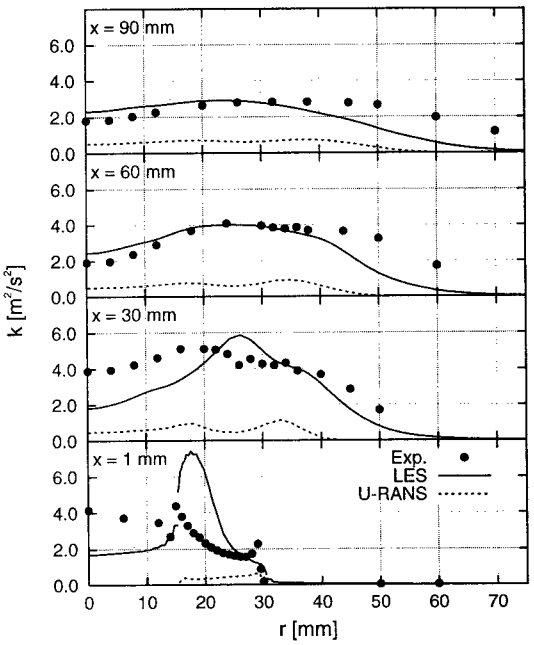

Figure 7: Radial profiles of time averaged turbulent kinetic energy at several axial positions for the $30kW$ case.

structure in one PVC cycle. Hence the doubled frequency.

Since computation of an energy spectrum is not possible for the U-RANS, velocity time series recorded at selected points of the flow field were Fourier transformed directly. The result of this procedure is shown in figure 12. For the Fourier analysis of the U-RANS, the spectral resolution was quite coarse (approx. 10% when related to the peak frequency). This is due to the fact that only two vortex core periods were analysed. But within that range of uncertainty the precession frequencies are predicted with remarkable accuracy when compared to the experimental data.

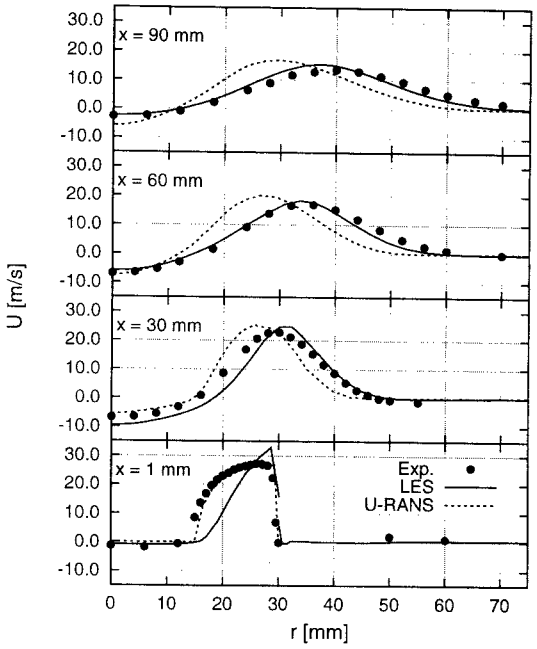

Figure 8: Radial profiles of time averaged axial velocity at several axial positions for the $150kW$ case.

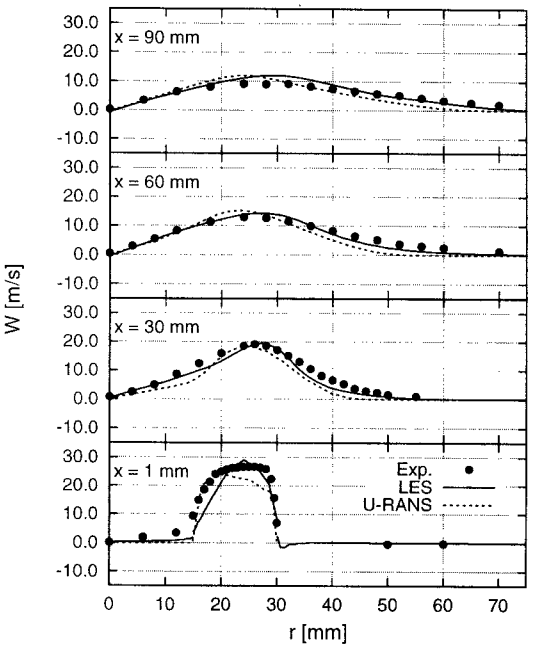

Figure 9: Radial profiles of time averaged azimuthal velocity at several axial positions for the $150kW$ case.

In figure 13, the peak frequency for the two cases are plotted as a function of Reynolds number.

The precession frequency can also be defined in terms of the Strouhal number defined as $St = \tau \cdot U/L$, where τ is the inverse of the peak frequency and the characteristic velocity U and length L are the same as were used for computing the Reynolds number. For a given flow configuration the Strouhal number is expected to reach an asymptotic value in the limit of high Reynold numbers. The precession frequency then increases linearly with the flow rate (Gupta et al. (1984)). This behavior seems to be correctly captured

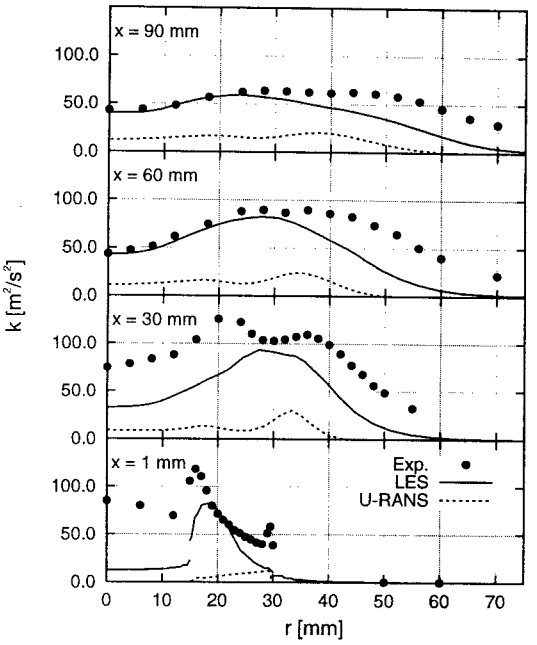

Figure 10: Radial profiles of time averaged turbulent kinetic energy at several axial positions for the $150kW$ case.

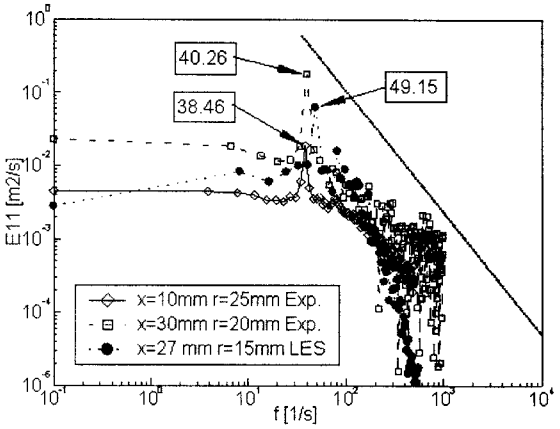

Figure 11: Turbulent energy spectra computed from temporal autocorrelations obtained from the experiments and LES of the $30kW$ case. The dotted line indicates the $k^{-5/3}$ decay of energy.

by the U-RANS. From the experiment a value of $St \approx 3.81$ was obtained. The U-RANS predicted a slightly higher value of $St \approx 3.95$. It has to be mentioned though, that not enough data is available at the moment, to be sure that the asymptotic range is already reached. It is also not clear yet, why the LES delivers differing frequencies.

CONCLUSIONS

So far it could be confirmed that the U-RANS method is able to capture the precessing vortex core phenomenon both qualitatively and quantitativeley. Good agreement of mean quantities was achieved when comparing the U-RANS results to experimental data and LES computations. The level of fluctuations and the spreading rate of the flow were underpredicted by the U-RANS.

It should be mentioned that for 3-d time dependent simu-

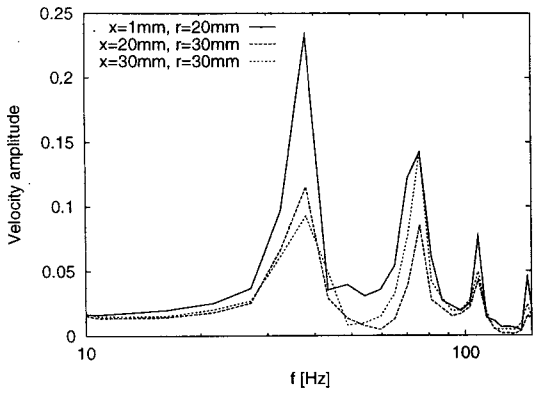

Figure 12: Fourier transform of velocity from the U-RANS of the $30kW$ case.

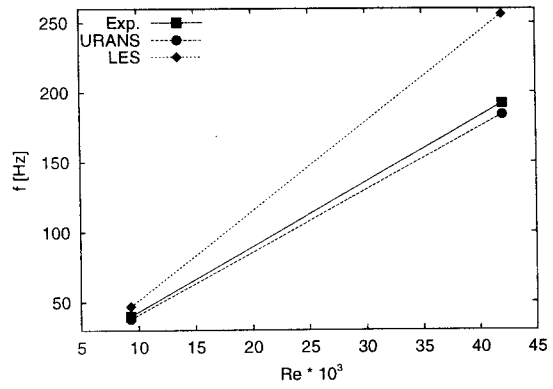

Figure 13: Dimensionless peak precessing vortex core frequency plotted over Reynolds number.

lations as performed in the present study the computational cost is significantly increased when compared to steady state RANS computations. The use of algebraic Reynolds stress models instead of the differential model used in this paper might prove useful in this regard, but is left as future work. Computational requirements are still low when compared with those for LES.

ACKNOWLEDGEMENTS

The authors gratefully acknowledge the *Deutsche Forschungsgemeinschaft* for financial support through SFB 568 "Flow and Combustion in Future Gas Turbine Combustion Chambers" and GK 91 "Modelling and Numerical Description of Technical Fluid Flows".

REFERENCES

Bowen, P. J., O'Doherty, T. and Lucca-Negro, O. (1998), "Rotating Instabilities in Swirling and Cyclonic Flows, Part B: Theoretical Analysis," in "Thermal Energy Engineering and the Environment," (D. Zhang and G. Nathan, eds.), pp. 197–220, The University of Adelaide, Department of Chemical Engineering, Adelaide.

Chanaud, R. C. (1965), "Observations of Oscillatory Motion in Certain Swirling Flows," *J. Fluid Mech.*, Vol. 21(1):111–127.

Derksen, J. J. and den Akker, H. E. A. V. (2000), "Simulation of Vortex Core Precession in a Reverse-Flow Cyclone," *AIChE Journal*, Vol. 46(7):1317–1331.

Durbin, P. A. (2002), "A Perspective on Recent Developments in RANS Modeling," in "Engineering Turbulence Modelling and Experiments 5," (W. Rodi and N. Fueyo, eds.), pp. 3–16, Elsevier Science Ltd.

Düsing, M., Sadiki, A. and Janicka, J. (2002), "LES of Confined Methane-Air Diffusion Flames Using Oscillating Inflow Conditions," in "Engineering Turbulence Modelling and Experiments 5," (W. Rodi and N. Fueyo, eds.), pp. 907–926, Elsevier Science Ltd.

Guo, B., Langrish, T. A. G. and Fletcher, D. F. (2002), "CFD simulation of precession in sudden pipe expasnion flows with low inlet swirl," *Applied Mathematical Modelling*, Vol. 26:1–15.

Gupta, A. K., Lilley, D. G. and Syred, N. (1984), *Swirl Flows*, Abacus Press, Tunbridge Wells, Kent.

Jones, W.-P. (1994), "Turbulence Modeling and Numerical Solution Methods for Variable Density Flows," in "Turbulent Reacting Flows," (P. Libby and F. Williams, eds.), pp. 309–347, Academic Press, London, San Diego, New York.

Leibovich, S. (1978), "The structure of vortex breakdown," *Annu. Rev. Fluid Mech*, Vol. 10:221–246.

Lilly, D. K. (1992), "A Proposed Modification of the Germano Subgrid-Scale Closure Method," *Phys. Fluids*, Vol. 4(3):633–635.

Lucca-Negro, O. and O'Doherty, T. (2001), "Vortex breakdown: a review," *Prog. Energy Combust. Sci.*, Vol. 27(4):431–481.

Mengler, C., Heinrich, C., Sadiki, A. and Janicka, J. (2001), "Numerical Prediction of momentum and scalar fields in a jet in cross flow: Comparison of LES and second order turbulence closure calculations," in "Turbulent Shear Flow Phenomena II," Vol. 2, pp. 425–431.

Pierce, C. D. and Moin, P. (1998), "A dynamic model for subgrid-scale variance and dissipation rate of a conserved scalar," *Phys. Fluids*, Vol. 10(12):3041–3044.

Schneider, C., Repp, S., Sadiki, A., Dreizler, A. and Janicka, J. (2001), "The effect of swirling number variation on turbulent transport and mixing processes in swirling recirculating flows: experimental and numerical investigations," in "Turbulent Shear Flow Phenomena II," Vol. 3, pp. 363–368.

Shir, C. C. (1973), "A preliminary study of atmospheric turbulent flows in the idealized planetary boundary layer," *J. Atm. Sci.*, Vol. 30:1327–1339.

Sloan, D. G., Smith, P. J. and Smoot, L. D. (1986), "Modeling of Swirl in Turbulent Flow Systems," *Prog. Energy Combust. Sci.*, Vol. 12:163–250.

Syred, N. and Beer, J. M. (1974), "Combustion in Swirling Flows: A Review," *Combustion and Flame*, Vol. 23:143–201.

Tang, G., Yang, Z. and McGuirk, J. J. (2002), "Large Eddy Simulation of Isothermal Confined Swirling Flow with Recirculation," in "Engineering Turbulence Modelling and Experiments 5," (W. Rodi and N. Fueyo, eds.), pp. 885–894, Elsevier Science Ltd.

Wegner, B., Kempf, A., Schneider, C., Sadiki, A., Dreizler, A., Schäfer, M. and Janicka, J. (2003), "Large Eddy Simulation of Combustion Processes under Gas Turbine Conditions," *Prog. Comput. Fluid Dynamics*, accepted for publication.